

## Quantitative Evaluation of Adsorption and Desorption Behavior of Carbon Dioxide over Perovskite-Type Oxides

Tsutomu Sakai, Atsushi Murata, Jun-ichiro Hayashi,  
Katsuki Kusakabe and Shigeharu Morooka

*Department of Chemical Science and Technology, Kyushu University, Fukuoka 812-81, Japan*

### Scope

Separation of CO<sub>2</sub> from effluent gas is important for global environmental protection. Activated carbon and silica gel are good adsorbents of CO<sub>2</sub> but they lose their ability at high temperature. On the other hand, perovskite compounds possess CO<sub>2</sub> adsorptivity at elevated temperature and can be used as CO<sub>2</sub> adsorbent. In the present study, several perovskite compounds with high specific area were synthesized by different methods and their CO<sub>2</sub> adsorptivity was determined. Adsorption/desorption rate of CO<sub>2</sub> was also evaluated by a pulse response method and a temperature-programmed desorption technique.

### Experimental

Perovskite compounds were synthesized by the following methods:

- (1) Nitrates precipitation: Aqueous solutions of nitrates were mixed, and water was slowly evaporated by heating.
- (2) Citrates precursor: Excess citric acid and ethylene glycol were added to an aqueous solution of nitrates. Water was evaporated in a rotary evaporator until a viscous liquid was obtained. The precursor was further dried in vacuum at 100°C.
- (3) Cyanides precipitation: La(NO<sub>3</sub>)<sub>3</sub>·6H<sub>2</sub>O and K<sub>3</sub>[Co(CN)<sub>6</sub>] were dissolved in water and mixed to get a precipitate at 60°C.
- (4) Diluted precipitation: An aqueous solution of nitrates was dropped slowly into a water-ethanol-ammonia solution. The gel was recovered by centrifugation.
- (5) Alkoxides sol-gel: An iso-propanol solution of Ba(iso-OC<sub>3</sub>H<sub>7</sub>)<sub>2</sub> and Ti(iso-OC<sub>3</sub>H<sub>7</sub>)<sub>4</sub> was hydrolyzed at 80°C. The hydrated oxide was dried in vacuum.

The calcination temperature was varied in 400–700°C and was optimized to attain both high crystallinity and surface area of powders. Solids were characterized with XRD, EDX and BET. The morphology of particles was observed with SEM.

Total adsorption of CO<sub>2</sub> was determined with TG. The temperature was increased at a rate of 5 K·min<sup>-1</sup> to 500°C. The total pressure was kept at 101 kPa. Dynamic CO<sub>2</sub> adsorption was evaluated for LaAlO<sub>3</sub> and BaTiO<sub>3</sub> by applying the impulse response method of gas chromatography. LaAlO<sub>3</sub> or BaTiO<sub>3</sub> powder was packed in a separation column through which argon flew as the carrier. Pulses of CO<sub>2</sub> and Ar mixture were injected every ten minutes into the column until a steady-state response curve was attained.

Dynamic CO<sub>2</sub> adsorption was also evaluated by applying the temperature programmed desorption. The carrier gas was helium containing 8 vol% of CO<sub>2</sub>. After adsorption equilibrium was attained, the column was heated at a rate of 3–20 K·min<sup>-1</sup> from 30°C to 550°C. The effluent gas was continuously introduced into a TCD-GC and the desorption rate was evaluated.

## Results and Discussion

The X-ray diffraction patterns shown in Fig. 1 reveal that the single phase LaFeO<sub>3</sub> crystal was obtained by the citrates precursor and diluted precipitation methods. Conditions of the other methods and crystallinity of products are summarized in Table 1. Figures 2 (a) and (b) respectively show the morphology of LaFeO<sub>3</sub> and LaAlO<sub>3</sub> particles prepared by the citrates precipitation method. Figures 3 (a) and (b) indicate their total CO<sub>2</sub> adsorption isotherms in a range of 25–500°C. The other perovskite compounds prepared show the similar tendency. CO<sub>2</sub> isotherms obeyed the Freundlich equation and the amount of adsorption was proportional to the 1/n power of CO<sub>2</sub> partial pressure. At a CO<sub>2</sub> partial pressure of 10 kPa, the amount of CO<sub>2</sub> adsorbed by LaFeO<sub>3</sub> was about 14 μmol·m<sup>-2</sup> at 25°C and roughly whole surface was covered by a monolayer of CO<sub>2</sub> molecules. It decreased to about 7 μmol·m<sup>-2</sup> at 500°C. Silica gel that adsorbed about 3.5 μmol·m<sup>-2</sup> of CO<sub>2</sub> at 25°C exhibited no adsorptivity at 500°C.

Figure 4 illustrates typical impulse response curves obtained with the chromatographic column packed with LaAlO<sub>3</sub>. The response curve was very broad at 100°C and peaks of N<sub>2</sub> and CO<sub>2</sub> were separated at 500°C. Thus a part of CO<sub>2</sub> molecules adsorbed at 500°C were mobile, but the mount of mobile CO<sub>2</sub> was not large. The mean residence time of CO<sub>2</sub> increased with increasing column temperature. This is quite different from the tendency with silica gel, whose adsorptivity decreased with increasing temperature.

Figure 5 shows TPD profiles of LaCoO<sub>3</sub>, LaFeO<sub>3</sub> and LaAlO<sub>3</sub>, suggesting widely distributed activation energies of adsorption. The maximum desorption rate was observed at 75–80°C for all samples tested. The total amount of CO<sub>2</sub> desorbed was determined by integrating the desorption rate between 30–550°C. The relationship among CO<sub>2</sub> coverage  $\theta$ , desorption rate  $(-\Delta\theta/\Delta t)/\theta$  and temperature  $T$  was obtained for different heating rates. Activation energy  $E$  and frequency factor  $k_0$  were defined by  $(-\Delta\theta/\Delta t)/\theta = k_0 \exp(-E/RT)$  and calculated from the Arrhenius plot of the desorption rate at a same CO<sub>2</sub> coverage.

As shown in Fig. 6, the activation energy for LaFeO<sub>3</sub> was 100–150 kJ/mol when the CO<sub>2</sub> coverage was smaller than 0.4 and decreased to 40–50 kJ/mol at larger CO<sub>2</sub> coverage in the lower temperature range. The frequency factor varied with the CO<sub>2</sub> coverage by five orders of

Table 1. Perovskite compounds prepared.

	Methods	Calcination temperature	Single phase	BET surface area [m <sup>2</sup> ·g <sup>-1</sup> ]
LaCoO <sub>3</sub>	Nitrates precipitation	800°C, 2h	X	-
	Citrates precursor	600°C, 2h	O	9.8
	Diluted precipitation	650°C, 4h	O	13.9
	Cyanides precipitation	650°C, 4h	X	16.8
LaFeO <sub>3</sub>	Nitrates precipitation	600°C, 2h	X	9.9
	Citrates precursor	600°C, 1h	O	22.8
	Diluted precipitation	600°C, 2h	O	7.2
LaAlO <sub>3</sub>	Citrates precursor	800°C, 1h	O	13.8
LaNiO <sub>3</sub>	Nitrates precipitation	800°C, 2h	X	-
	Citrates precipitation	800°C, 2h	O	3.6
LaCrO <sub>3</sub>	Nitrates precipitation	800°C, 2h	O	2.8
BaTiO <sub>3</sub>	Alkoxides sol-gel	600°C, 2h	O	47
	Alkoxides sol-gel	800°C, 2h	O	37

magnitude. The desorption rate  $(-\Delta\theta/\Delta t)/\theta$  at 500°C was of the order of  $10^{-2} \text{ s}^{-1}$  at a  $\text{CO}_2$  coverage of 0.5. This rate would be smaller than the permeation rate through a thin membrane for gas separation. Thus,  $\text{LaFeO}_3$  that was prepared in this study may not be competent as a membrane-constructing material. However, its desorption rate is acceptable when it is used as a packed-bed adsorbent. The results for  $\text{LaAlO}_3$  were fundamentally similar with those of  $\text{LaFeO}_3$ .

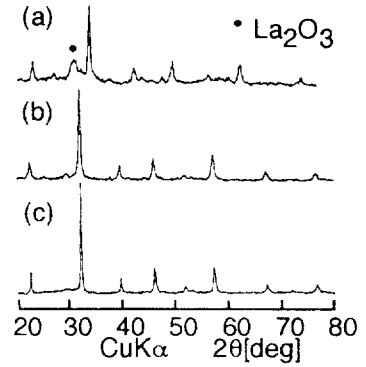


Figure 1. XRD patterns of  $\text{LaFeO}_3$ .  
 (a) Nitrates precipitation;  
 (b) citrates precursor; and  
 (c) diluted precipitation.

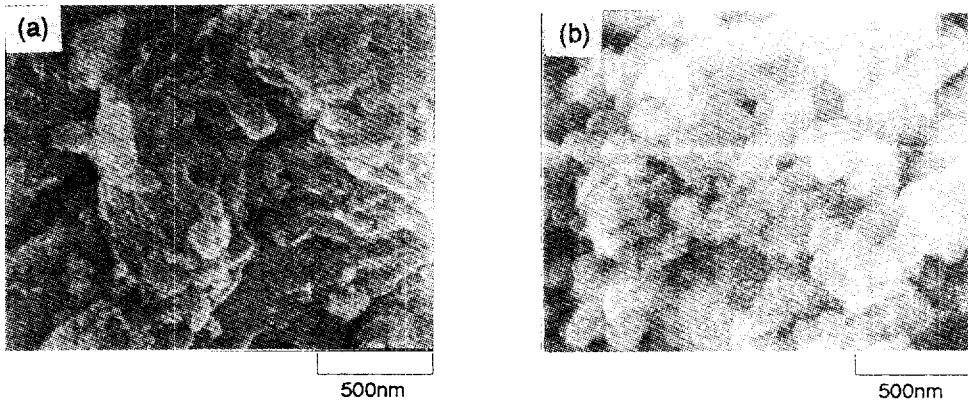


Figure 2. SEM images of perovskites; (a)  $\text{LaFeO}_3$  and (b)  $\text{LaAlO}_3$ .

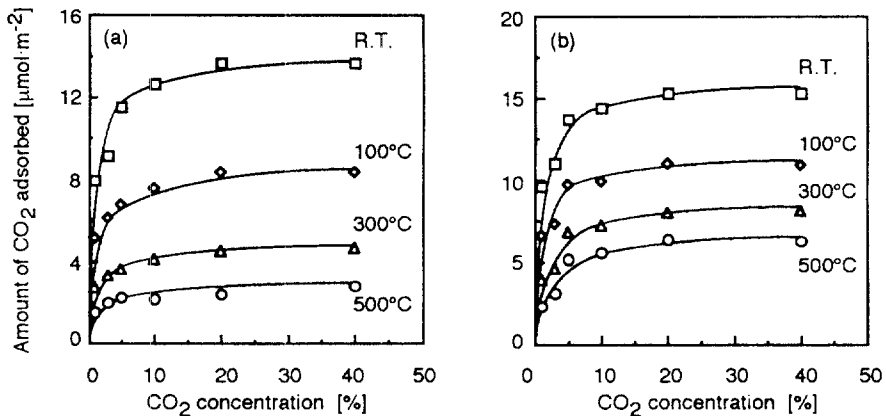


Figure 3. Adsorption isotherms of (a)  $\text{LaFeO}_3$  and (b)  $\text{LaAlO}_3$ .

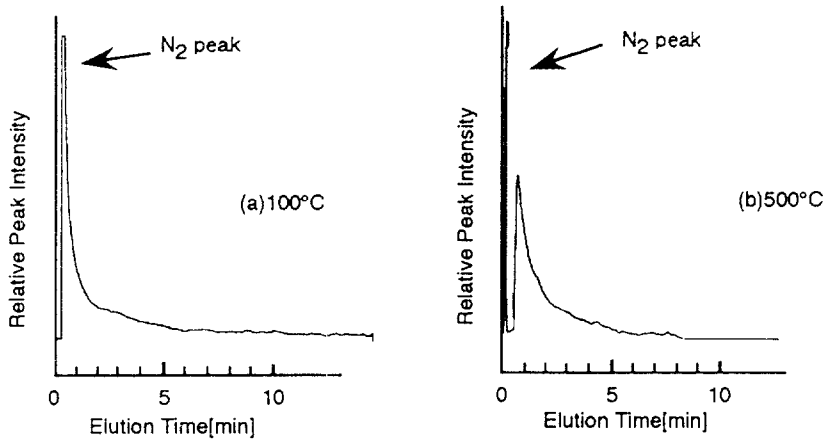


Figure 4. Impulse response curves of  $\text{CO}_2$  through  $\text{LaAlO}_3$  column

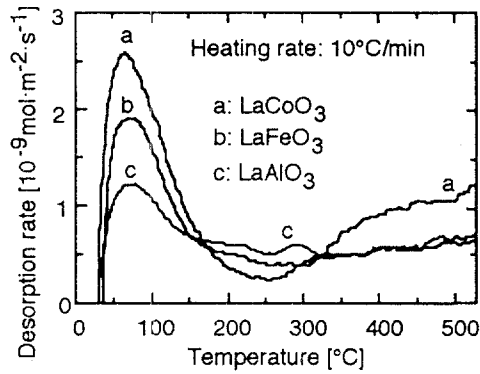


Figure 5. TPD profiles of  $\text{LaCoO}_3$ ,  $\text{LaFeO}_3$  and  $\text{LaAlO}_3$

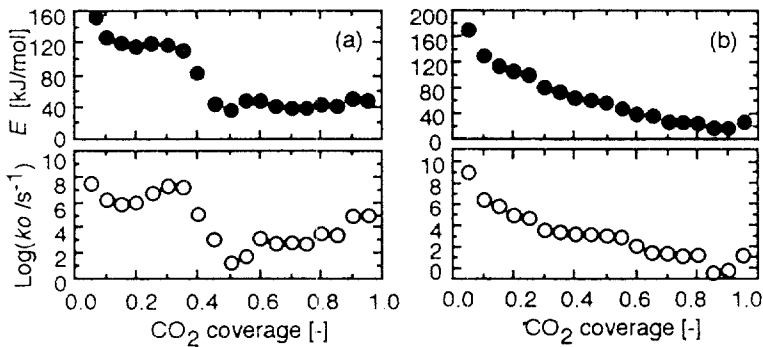


Figure 6. Effect of  $\text{CO}_2$  coverage of  $E$  and  $k_0$ .  
(a)  $\text{LaFeO}_3$  and (b)  $\text{LaAlO}_3$ .